

ELECTRON-CLOUD UPDATED SIMULATION RESULTS FOR THE PSR, AND RECENT RESULTS FOR THE SNS. *

M. Pivi and M. A. Furman,[†] LBNL, Berkeley, CA94720, USA

Abstract

We present recent simulation results for the main features of the electron cloud in the storage ring of the Spallation Neutron Source (SNS) at Oak Ridge, and updated results for the Proton Storage Ring (PSR) at Los Alamos. In particular, a complete refined model for the secondary emission process including the so called true secondary, rediffused and backscattered electrons has been included in the simulation code.

1 INTRODUCTION

The Spallation Neutron Source (SNS) under construction at the Oak Ridge National Laboratory (ORNL), has initiated studies on the possible electron-cloud effect, which may limit the performances of the proton storage ring. A similar high-intensity instability which has been observed in the PSR at the Los Alamos National Laboratory (LANL) for more than 13 years, is now recognized to be, although not conclusively proven, an electron-cloud effect. Since 1987 the PSR has reported a fast instability that is responsible for proton losses and collective beam motion above a certain current threshold, and is accompanied by a large number of electrons. This instability is now believed to be due to the collective coupling between an electron cloud and the proton beam [1, 2]. Such instability is a particular manifestation of the electron-cloud effect (ECE) that has been observed or is expected at various other machines. In this article we present simulation results for the SNS and for PSR ring obtained with the ECE code that has been developed at LBNL over the past 6 years, suitably augmented to deal with very long and intense bunches such as in the case of long proton beams. At the present stage, we have restricted our studies to look in detail at the dynamics of the electron cloud rather than the instability *per se*. Thus in all results presented here, the proton beam is assumed to be a static distribution of given charge and shape moving on its nominal closed orbit, while the electrons are treated fully dynamically. This approximation is valid for stable beam operation, and it is probably reasonable for mild instability. We defer issues like the current instability threshold, growth rate and frequency spectrum to future studies. We compared in [3] our results for the electron current and energy spectrum of the electrons hitting the walls of the chamber against measurements obtained in the PSR by means of dedicated electron probes. From such comparisons we can assess the effects of several important parameters such as the secondary electron yield (SEY) at

the walls of the chamber, the proton loss rate and electron yield, etc. Furthermore, we can infer details of the electron cloud in the vicinity of the proton beam, such as the neutralization factor, which is important for a self-consistent treatment of the coupled e-p problem [4].

Table 1: Simulation parameters for the PSR and SNS.

Parameter	Symbol	PSR	SNS
proton beam energy	E , GeV	1.735	1.9
dipole field	B , T	1.2	0.78
bunch population	N_p , $\times 10^{13}$	5	20.5
ring circumference	C , m	90	248
revolution period	T , ns	350	945
bunch length	b_l , ns	254	760
gauss. tr. bunch size	σ_x, σ_y , mm	10, 10	
flat tr. bunch size	r_x, r_y , mm		28, 28
beam pipe semi-axes	a, b , cm	5,5	10,10
proton loss rate	p_{loss} , $\times 10^{-6}$	4	0.11
proton-electron yield	Y ,	100	100
No. kicks/bunch	N_k	1001	5001
No. steps during gap	N_g	100	250
SEY params:			
max sec. yield	δ_{max}	2.0	2.0
energy at yield max	E_{max} , eV	300	300
yield low energy el.	$\delta(0)$	0.5	0.5

2 PHYSICAL MODEL

2.1 Sources of electrons

In this article we consider what we expect to be the main two sources of electrons for proton storage rings as the SNS and the PSR, namely: lost protons hitting the vacuum chamber walls, and secondary emission from electrons hitting the walls (we are not interested here in simulating the electron cloud in the vicinity of the stripper foil). Although our code accommodates other sources of electrons, such as residual gas ionization, we have turned them off for the purposes of this article.

2.2 Secondary emission process

We represent the SEY $\delta(E_0)$ and the corresponding emitted-electron energy spectrum $d\delta/dE$ (E_0 =incident electron energy, E = emitted secondary energy) by a detailed model described elsewhere [5]. Its parameters were obtained from detailed fits to the measured SEY of stainless steel (St. St.) [6]. The main SEY parameters are

* Work supported by the SNS project and by the US DOE under contract DE-AC03-76SF00098.

[†] mpivi@lbl.gov and mafurman@lbl.gov

the energy E_{max} at which $\delta(E_0)$ is maximum, and the peak value itself, $\delta_{max} = \delta(E_{max})$ (see Table 1). Furthermore, for the results shown below, we do take into account the elastic backscattered and rediffused components of the secondary emitted-electron energy spectrum $d\delta/dE$. The backscattered component typically becomes more important at low incident electron energies. To account for this behavior we have used a fit extrapolated data for copper measured at CERN [7].

The value of $\delta(E_0)$ at incident electron energies $E_0 < 10eV$ is an important parameter since it determines the electron accumulation rate, and also the electron survival rate at the end of the gap. This quantity is difficult to measure experimentally, and remains an uncertainty for the model. In our simulations we have made the assumption that $\delta(0) \simeq 0.5$. In this case, the simulated electron density increases by a factor ~ 3 and the peak detector current by almost a factor ~ 2.5 , relative to the $\delta(0) \simeq 0.1$ case (refer to previous results for PSR with no rediffused nor backscattered electrons, see [3]). These are examples of strong parameter sensitivity that calls for further experimental investigations.

2.3 Simulation Model

The SNS and the PSR rings store a single proton bunch of length τ_b followed by a gap of length τ_g with a typical current intensity profile shown in Figs. 2 and 4. In our simulation we assume a Gaussian transverse PSR beam with rms sizes $\sigma_x = \sigma_y = 10mm$, and we use the actually measured longitudinal intensity profile. A flat transverse beam with $r_x = r_y = 28mm$ is assumed for the SNS. We simulate the passage of the proton bunch in a field-free region with a vacuum chamber which we take to be a cylindrical perfectly-conducting pipe. The number of electrons generated by lost protons hitting the vacuum chamber wall is $N_p \times Y \times p_{loss}$ per turn for the whole ring, where Y is the effective electron yield per lost proton, and p_{loss} is the proton loss rate per turn for the whole ring per beam proton. We assume the lost-proton time distribution to be proportional to the instantaneous bunch intensity. The electrons are then simulated by macroparticles. The secondary electron mechanism adds to these a variable number of macroparticles, generated according to the SEY model mentioned above. The bunch is divided up into slices, so that the macroparticles experience N_k kicks during the bunch passage. We divide the interbunch gap into N_g intermediate steps. The space charge force is computed and applied at each slice in the bunch and each step in the gap. The image forces from both protons and electrons are taken into account, assuming a perfectly conducting wall. Typical parameter values are shown in Table 1.

3 RESULTS AND DISCUSSION

The possible amplification mechanism which may take place in long-beam machines is explained in Fig. 1. An electron present in the vacuum chamber before the bunch

passage oscillates in the beam well potential, and it is released at the end of the beam passage. Instead, electrons generated at the wall by proton losses at the maximum of the beam pulse are accelerated and decelerated by the beam potential and hit the opposite wall with a net energy gain, producing secondary electrons.

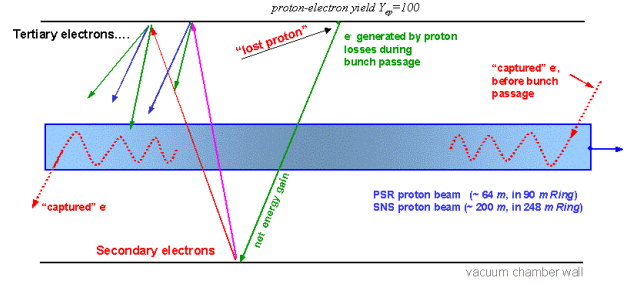


Figure 1: Electron multiplication mechanism in long proton bunches.

Electrons which survive the gap between two bunch passages will increase in number. The electrons gradually increase in number during successive bunch passages until, owing to the space-charge forces, a balance is reached between emitted and absorbed electrons. The build-up of the electron cloud in a PSR field-free region and a dipole section during the passage of the beam is shown in Fig. 2. The saturation level in the PSR is reached after few bunch passages, when assuming $\delta_{max} = 2$. The estimated average number of electrons in a field free region is $\sim 4 \times 10^7 e^-/cm^3$ or $50nC/m$. The neutralization factor or fractional charge neutralization, ratio e^-/p^+ , during a bunch passage is shown in Fig. 3.

The SNS beam pipe chamber will be coated with TiN, and recent measurements of an *as-received* SNS sample of the TiN coated vacuum chamber, has shown $\delta_{max} = 2$ [8]. Consistent results were obtained at KEK [9]. The build-up of the electron cloud in the SNS field-free region and a dipole section during the passage of the beam is shown in Fig. 4 for $\delta_{max} = 2$. Due to a large electron multiplication, we have used a very low initial number of macroparticles per bunch passage. The simulations present a significant fluctuation in the turn-by-turn electron density, and we are going to refine the code to accomplish for the SNS case. Simulation results for the SNS [10] show a qualitative agreement, but a lower estimated electron density. The neutralization factor during a bunch passage is shown in Fig. 5. The tune shift due to electron neutralization of a factor ~ 1 may be estimated, for example, at 25% beam intensity, by

$$dQ_{ec} = -0.25 f \gamma^2 dQ_{sc} \sim -2 dQ_{sc} = -0.4 \quad (1)$$

where $dQ_{sc}=0.2$ is the space charge tune shift, $\gamma = 2.066$ is the usual relativistic factor of the beam, and f is the neutralization factor. Once the secondary electron yield has decreased to 1.3 and 1.1, we were able to increase signif

icantly the number of macroparticles to account for better statistics. The build-up of the electron cloud during the first few bunch passages is shown in Fig.6.

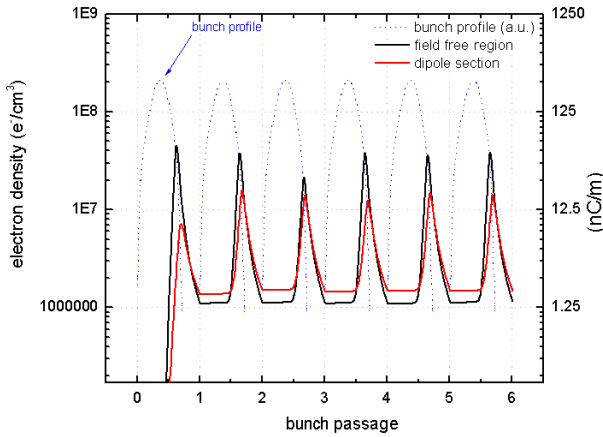


Figure 2: Simulated electron density during the first bunch passages, in a PSR field-free region and a dipole section. The saturation level is reached after few bunch passages.

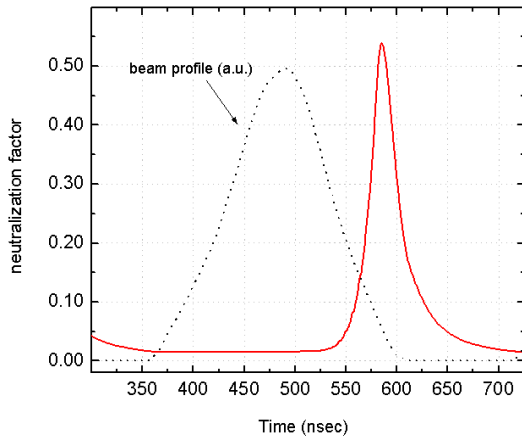


Figure 3: Simulated electron neutralization factor in a PSR field-free region, the fractional charge neutralization reaches 50% at the tail of the bunch.

4 CONCLUSION

A complete refined model for the secondary emission including the so-called true secondary, rediffused and backscattered electrons has been recently included in the code. We present an update of computer simulation results for the main features of the electron cloud at the Proton Storage Ring (PSR) and recent simulation results for the Spallation Neutron Source (SNS). Preliminary simulations for the SNS, show that a density of $\geq 150 \text{ nC/m}$ may be reached in a field-free region, leading to a significant tune shift given by electron neutralization. Due to a large unexpected electron multiplication in the case of the SNS, we have used a low number of macroparticles per bunch pas-

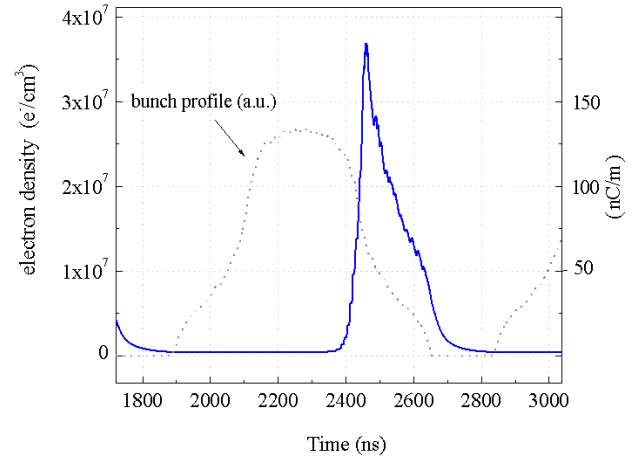


Figure 4: Simulated electron density during the first bunch passages, in a SNS field-free region.

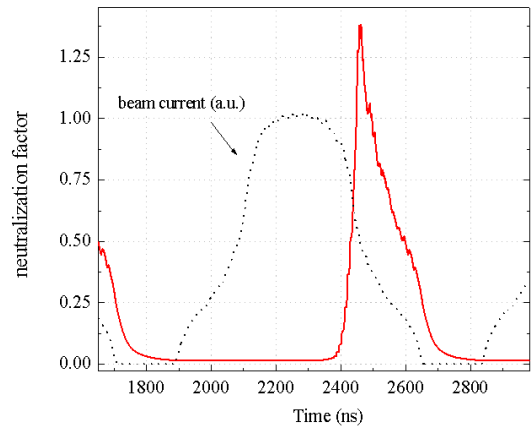


Figure 5: Simulated electron neutralization factor in a SNS field-free region, the fractional charge neutralization exceeds 1 at the tail of the bunch.

sage. The code is going to be implemented to accomplish for the SNS case.

5 ACKNOWLEDGEMENTS

We are particularly grateful to our colleagues of the PSR Instability Studies Program for many stimulating discussions, M. Blaskiewicz, K. Harkay, R. Davidson, H. Qin, P. Channell, T. S. Wang. We are especially grateful to R. Macek for discussions and for providing us the experimental data. Thanks to Y.H. Cai, F. Zimmermann, N. Hilleret, J. Wei, A. Wolski, S. Heifets, T. Raubenheimer, R. Kirby, A. Alexandrov, V. Danilov. We are grateful to NERSC for supercomputer support.

6 REFERENCES

- [1] For a summary, see: Proc. *ICFA Workshop on Two-Stream Instabilities*, Santa Fe, NM, US, Feb. 16-18, 2000, <http://www.aps.anl.gov/conferences/icfa/two->

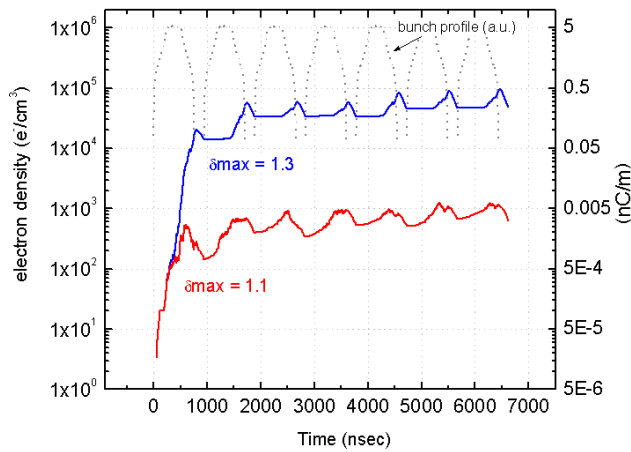


Figure 6: Build-up of the electron cloud in the SNS field-free region assuming a $\delta_{max} = 1.3$ and 1.1. The electrons gradually increase in number during successive bunch passages until, owing to the space-charge forces, a balance is reached between emitted and absorbed electrons.

stream.html, or also *International Workshop on Two-Stream Instabilities in Particle Accelerators and Storage Rings*, at KEK Tsukuba, Japan, September 11-14, 2001, <http://conference.kek.jp/two-stream/>.

- [2] R. Macek, these proceedings.
- [3] M. Furman and M. Pivi, Proc. PAC01, Chicago, IL, p. 708.
- [4] For an updated on the self consistent treatment of the instability see, for example, Physical Review Special Topic, *Special Collection Edition on Electron Cloud and Two-Stream Interactions in Long-Bunch Proton Beams*, future publication.
- [5] M. A. Furman and M. Pivi *Microscopic Probabilistic Model for the Simulation of the Secondary Electron Emission*, LBNL-49711, CBP Note-415, to be submitted to Physics Review ST, May 2002.
- [6] R. Kirby, private communication.
- [7] V. Baglin, I. Collins, B. Henrist, N. Hilleret, G. Vorlauffer, *A Summary of Main Experimental Results Concerning the Secondary Electron Emission of Copper*, LHC-Project-Report-472.
- [8] M. Blaskiewicz, private communication, May 2002.
- [9] T. Toyama, K. Ohmi, *Study for ep Instability in High Intensity Proton Ring*, these proceedings.
- [10] M. Blaskiewicz *Electron Cloud in the PSR and SNS* these proceedings.